Calmodulin Contributes to Gating Control in Olfactory Calcium-activated Chloride Channels

Hiroshi Kaneko, Frank Möhrlen, and Stephan Frings

Department of Molecular Physiology, University of Heidelberg, 69120 Heidelberg, Germany

In sensory neurons of the peripheral nervous system, receptor potentials can be amplified by depolarizing Cl currents. In mammalian olfactory sensory neurons (OSNs), this anion-based signal amplification results from the sequential activation of two distinct types of transduction channels: cAMP-gated Ca channels and Ca-activated Cl channels. The Cl current increases the initial receptor current about 10-fold and leads to the excitation of the neuron. Here we examine the activation mechanism of the Ca-dependent Cl channel. We focus on calmodulin, which is known to mediate Ca effects on various ion channels. We show that the cell line *Odora*, which is derived from OSN precursor cells in the rat olfactory epithelium, expresses Ca-activated Cl channels. Single-channel conductance, ion selectivity, voltage dependence, sensitivity to niflumic acid, and Ca sensitivity match between *Odora* channels and OSN channels. Transfection of *Odora* cells with CaM mutants reduces the Ca sensitivity of the Cl channels. This result points to the participation of calmodulin in the gating process of Ca-ativated Cl channels, and helps to understand how signal amplification works in the olfactory sensory cilia. Calmodulin was previously shown to mediate feedback inhibition of cAMP-synthesis and of the cAMP-gated Ca channels in OSNs. Our results suggest that calmodulin may also be instrumental in the generation of the excitatory Cl current. It appears to play a pivotal role in the peripheral signal processing of olfactory sensory information. Moreover, recent results from other peripheral neurons, as well as from smooth muscle cells, indicate that the calmodulin-controlled, anion-based signal amplification operates in various cell types where it converts Ca signals into membrane depolarization.

The Journal of General Physiology

INTRODUCTION

Anion-based signal amplification serves to boost Ca-induced membrane depolarization through activation of Cl currents. It was first examined in smooth muscle cells where cytosolic Ca signals, induced by Ca influx or release, trigger the opening of Ca-activated Cl channels. Because of the high cytosolic Cl concentration in smooth muscle cells, Cl efflux depolarizes the membrane and promotes the opening of voltage-gated Ca channels and, hence, contraction (for review see Leblanc et al., 2005). A growing body of evidence suggests that anion-based signal amplification also operates in neurons of the peripheral nervous system, including olfactory sensory neurons (OSN; for review see Frings, 2001) and somatic and visceral primary afferents (Kenyon and Goff, 1998; Oh and Weinreich, 2004; Lee et al., 2005). The amplification mechanism is probably best understood in OSNs. These primary sensory neurons detect odorants in the inhaled air by their cilia, and all components of the signal transduction cascade are present in these chemosensory organelles. The ciliary membrane contains Ca-permeable transduction channels that are gated by the second messenger cAMP (Nakamura and Gold, 1987), as well as Ca-activated Cl channels, expressed at eightfold higher density (Kleene and Gesteland, 1991; Reisert et al., 2003). Moreover, Cl^- uptake mechanisms maintain an elevated ciliary Cl concentration and thereby support depolarizing Cl efflux (Kaneko et al., 2004; Reisert et al., 2005; Nickell et al., 2006). These components set the scene for anion-based signal amplification; the Ca influx through cAMP-gated channels triggers a much larger Cl efflux and thereby ensures the generation of a depolarizing receptor potential sufficient for electrical excitation.

While this concept has been discussed for several years (Kleene, 1993; Kurahashi and Yau, 1993; Lowe and Gold, 1993), some key information about the interplay between the two transduction channels in the ciliary membrane has only recently become available. These data concern the Ca conductance, subunit composition, and regulation of the cAMP-gated channels (Dzeja et al., 1999; Bradley et al., 2004; Zheng and Zagotta, 2004), the functional properties of the olfactory Ca-activated Cl channels (Kleene, 1997; Reisert et al., 2003), as well as the regime of Cl homoeostasis in OSNs (Reuter et al., 1998; Kaneko et al., 2004; Reisert et al., 2005). Presently, the major obstacle to further explorations of anion-based signal amplification is the lack of information about the molecular identity of the Ca-activated Cl channels. The currently known families of Ca-activated Cl channels, the CLCA and bestrophin

Correspondence to Stephan Frings: s.frings@zoo.uni-heidelberg.de

Abbreviations used in this paper: DRG, dorsal root ganglia; OSN, olfactory sensory neuron; PDE, phosphodiesterase; RFP, red fluorescent protein.

families (for reviews see Hartzell et al., 2005; Loewen and Forsyth, 2005), seem to be poor candidates, because neither their expression patterns nor their functional properties are consistent with the native Cl channels in OSNs. In this situation we need to know more about the channels, particularly about the way cytosolic Ca controls their gating.

In most Ca-regulated ion channels, Ca does not bind directly to the channel protein, but Ca effects are mediated by calmodulin (CaM), which can be permanently associated with the channel as a Ca-sensing subunit (for review see Saimi and Kung, 2002). To examine if such an interaction also exists between CaM and the olfactory Ca-activated Cl channel, we expressed engineered CaM mutants and studied their effects on the activation of Ca-dependent Cl currents. We used the cell line *Odora* for this study, which was derived from rat OSN precursor cells (Murrell and Hunter, 1999). We examined Ca-activated Cl channels in *Odora* cells to compare their functional properties with native channels in OSNs. To probe for an involvement of CaM in channel activation, we measured the Ca sensitivity of Cl channels in *Odora* cells expressing CaM mutants.

MATERIALS AND METHODS

Odora cells were supplied by D. Hunter (Tufts University, Boston, MA) and cultivated in minimum essential medium (M2279; Sigma-Aldrich), supplemented with 10% FBS (F7524; Sigma-Aldrich), 1% penicillin/streptomycin (G6784; Sigma-Aldrich), and 1% nonessential amino acids (M7145; Sigma-Aldrich), at 33°C, 7% CO_2. These conditions maintain the "control" state of the cell line (Murrell and Hunter, 1999), and all results obtained in the present study were obtained from cells in that state. Because the cell line was originally transformed using a temperature-sensitive mutant (tsA58) of the SV40 large T antigen, the cells respond to increased temperature (39°C) with a change in protein expression pattern. This change is supported by 1 μg/ml insulin, 20 μM dopamine, and 100 μM ascorbic acid, included in the culture medium (Murrell and Hunter, 1999). In our hands, *Odora* cells showed an increased level of expression for adenylyl cyclase III and $G\alpha_{olf}$ after that treatment. Expression of Ca-activated Cl channels, however, was not significantly enhanced. For this reason, and because transfection efficiency was higher in the control state (5–10%), we used untreated cells for this study. All *Odora* cells in the control state expressed Ca-activated Cl channels at levels sufficient for whole-cell patch-clamp recording.

The CaM mutants in pcDNA3 (Erickson et al., 2001) were provided by D.T. Yue (Johns Hopkins University School of Medicine, Baltimore, MA). EF-hand Ca binding sites of CaM were disabled by D→A exchanges: EF-hand 1: D20A; EF-hand 2: D56A; EF-hand 3: D93A; EF-hand 4: D129A (Keen et al., 1999). Cells were cotransfected by Ca-phosphate coprecipitation with plasmids encoding either CaM mutants or red fluorescent protein (RFP) as a marker. The approximate molar ratio of the CaM:RFP plasmid mixture was 2. The RFP vector was created by subcloning the KpnI/NotI fragment of pDsRed (CLONTECH Laboratories, Inc.) into pcDNA3.1 (Invitrogen) providing the CMV promoter for expression in mammalian cells. 76% of the RFP-positive cells also expressed the recombinant CaM, as examined by coexpressing RFP with a YFP-tagged CaM version, and all RFP-positive cells examined expressed Ca-activated Cl channels. In the patch-clamp experiment, transfected cells were identified by the RFP fluorescence. The amount of heterologously expressed CaM in individual cells could not be established.

Western Blot Analysis

Membrane proteins were extracted from *Odora* cells by a modification of a previously described method (Bönigk et al., 1999) with ice cold lysis buffer containing (in mM) 10 NaCl, 2 EDTA, 25 HEPES, pH 7.5, and mammalian protease inhibitor mix G (Serva). The membrane pellet was washed in ice cold solution containing (in mM) 500 NaCl, 2 EDTA, 25 HEPES, pH 7.5 (including protease inhibitors), and resuspended in Laemmli buffer. Aliquots containing 15 μg of protein were subjected to SDS-PAGE on an 8% gel, transferred to a PVDF membrane (Masherey and Nagel), which was blocked with 5% milk powder in PBS. The blots were probed with anti adenylyl cyclase III (sc-588; Santa Cruz Biotechnology, Inc.) or anti $G_{\alpha\ s/olf}$ (sc-383; Santa Cruz Biotechnology, Inc.) primary antibodies. Appropriate secondary antibodies were HRP coupled and detected by the ECL Plus Western blotting system (GE Healthcare).

Electrophysiology and Single-cell Fluorescence

For electrophysiological experiments, transfected cells were transferred to poly-L-lysine–coated coverslips and used 24–48 h after plating. RFP-expressing cells were selected for whole-cell patch-clamp recording, filled with caged-Ca and fluo-5F, and kept in a solution containing (in mM) 50 NaCl, 90 Na-gluconate, 10 EGTA, 10 HEPES, pH 7.4 (NaOH). The pipette was filled with a solution containing (in mM) 140 CsCl, 1.5 $CaCl_2$, 1 $MgCl_2$, 0.15 EGTA, 10 HEPES, 5 DM-nitrophen (Calbiochem), 20 μM fluo-5F (Molecular Probes); pH 7.2 (CsOH). For measurements at +40 mV, the Cl gradient was reversed. The pipette solution contained (in mM) 50 CsCl, 90 Cs-gluconate, 1,5 $CaCl_2$, 1 $MgCl_2$, 0.15 EGTA, 10 HEPES, 5 DM-nitrophen, and 20 μM fluo-5F, pH 7.2 (CsOH); the bath contained (in mM) 140 NaCl, 10 EGTA, 10 HEPES, pH 7.4 (NaOH). The composition of these solutions was designed for low free Ca concentration (≤0.1 μM) before and high free Ca concentration (≥10 μM) after photorelease of caged Ca. The use of Cs excludes current contributions from Ca-activated K channels. 10 min were allowed after whole-cell breakthrough for equilibration between cytosol and pipette solution. Currents were recorded using a List EPC-7 patch-clamp amplifier (HEKA Elektronik) and an ISO2 recording system (MFK). The whole-cell resistance of *Odora* cells ranged between 100 and 1,000 MΩ, the capacitance was 15–40 pF. Single-cell fluorescence was recorded through a 40×/NA1.2 oil immersion lens and guided through the side port of an inverted microscope (Nikon Diaphot) to a photomultiplier (Thorn EMI Elecron Tubes) whose output was fed into the ISO2 system. Both excitation light (λ_{exc} = 470 nm) and fluorescence emission (λ_{em} = 520–560 nm) were restricted to the central aspect of the cell by adjustable masks in the optical pathway. Thus, fluorescence from the recording pipette, as well as fluorescence from thin cell protrusions were excluded. Light flashes for photolysis were produced by a 100-W Hg lamp (AMKO), timed by an electronically actuated shutter (Uniblix) and focused through the objective lens onto the cells. Long-duration flashes (500–1,000 ms) were used to produce large Ca steps, series of 50-ms flashes for quantitative evaluation of photorelease. The light path to the PMT was closed during the flash, causing a gap in the fluorescence trace. Control measurements showed that the light flashes did not cause any current deflection or fluorescence increments when caged Ca was excluded from the pipette solution. The free Ca concentration [Ca] was calculated from the measured single cell fluorescence using the equation

$$[Ca] = K_D \frac{F - F_{min}}{F_{max} - F}.$$

F_{min} is the fluorescence before the light flashes, and F_{max} was measured after saturation of the dye. Dye saturation at the end of the flash series was confirmed by adding 10 μM of the Ca ionophore ionomycin to the bath solution, which caused no further increase of cell fluorescence. The apparent dissociation constant K_D of fluo-5F in the presence of caged Ca was determined using a fluorescence spectrophotometer (Perkin Elmer, LS 50) and a Ca electrode. Reference solutions for the determination of Ca concentrations was the CALBUF-1 series (10^{-8}–10^{-1} M Ca; WPI), which was used to calibrate the Ca electrode.

RESULTS

Ca-activated Cl channels in *Odora* cells

Odora cells were cultivated at 33°C/7% CO_2, conditions that promote cell proliferation (Murrell and Hunter, 1999) and are conducive to transient transfection. Expression of marker proteins for the olfactory signal transduction cascade (adenylyl cyclase III, G_{olf}) was confirmed by Western blot analysis (Fig. 1 A). Since the molecular identity of olfactory Ca-activated Cl channels is not known, we used an assay that detects the generation of Cl currents arising in response to an increase of the intracellular Ca concentration. We applied Ca concentration jumps in *Odora* cells, triggered by photorelease of Ca from DM-nitrophen (caged Ca). To monitor the intracellular Ca concentration, we added to the pipette solution 20 μM fluo-5F, a Ca-sensitive fluorescent dye with a nominal dissociation constant K_D of 2.3 μM, comparable to the $K_{1/2}$ established for native Ca-activated Cl channels in rat OSNs (1–2 μM; Reisert et al., 2003). Fig. 1 B shows simultaneous current and fluorescence recordings elicited by photorelease of Ca in an *Odora* cell at −40 mV. Similar currents were recorded in all of 11 cells tested, the mean amplitude was −524 ± 106 pA (SD = 350 pA). To examine whether the *Odora* channels and Ca-activated Cl channels of rat OSNs have the same functional properties, we analyzed pharmacology, voltage dependence, anion selectivity, single-channel conductance, and Ca sensitivity of *Odora* channels and compared them to the properties of native channels in rat OSNs (Reisert et al., 2003). The data from *Odora* cells had to be obtained in the whole-cell configuration because the low channel density ruled out accurate analysis in excised patches. The mean current density was 19.5 pA/pF, and currents in inside-out patches were <2 pA. Niflumic acid, an analgesic and anti-inflammatory drug that blocks the OSN Cl channels at 100–300 μM (Lowe and Gold, 1993; Reisert et al., 2003), also suppressed the Ca-induced current in *Odora* cells reversibly (>90% block at 100 μM; three experiments). Fig. 1 C shows a whole-cell experiment where slow dialysis of an *Odora* cell with 3.5 μM free Ca induced a current that was blocked by 70% in the presence of 20 μM niflumic acid (six experiments). Dialysis with Ca-free solution did not induce current (not depicted). The native Cl channel in OSNs is highly anion selective with a clear

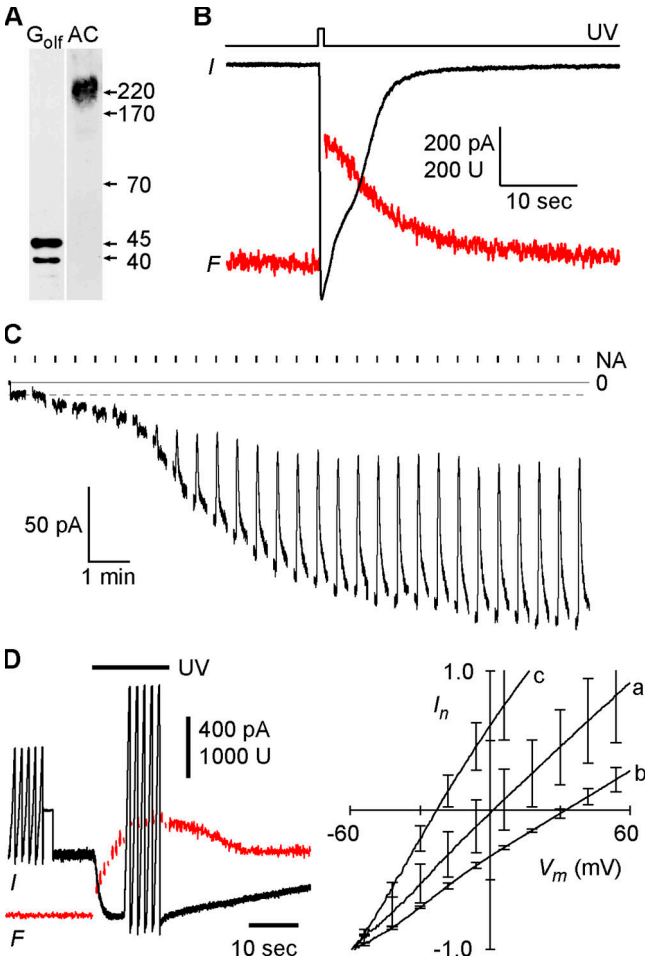

Figure 1. Ca-activated Cl currents in *Odora* cells. (A) Western blot of *Odora* cell membrane proteins showing expression of adenylyl cyclase type III (AC) and the olfactory GTP binding protein G_{olf}. (B) Simultaneous recording of whole-cell current (black trace) and Ca-dependent fluorescence (red trace) during flash-induced photorelease of Ca. The flash duration was 500 ms, V_m was −40 mV. (C) Sensitivity of the Ca-induced current to niflumic acid (NA). Whole-cell recording of an *Odora* cell during dialysis of the cytosol with a solution containing 3.5 μM free Ca and 140 mM CsCl. Immediately after breakthrough, the holding voltage was switched to −40 mV. The resulting leak current was about −9 pA (dashed line). As Ca diffused into the cell, the Cl current developed over 10 min up to a maximal amplitude of −160 pA. A 2-s pulse of 20 μM NA was delivered every 40 s. NA did not affect the leak current (first five pulses), but blocked 70% of the Ca-induced current. (D) To obtain I-V_m relations for the Ca-dependent channels, whole-cell currents were recorded during five voltage ramps (−60 to +60 mV) before and after photolysis of caged Ca. The averaged I-V_m relations recorded before illumination were subtracted from the I-V_m relations recorded during the maximal Ca signal. The resulting curves were normalized to their current values at −60 mV and superposed for symmetrical Cl concentrations (a, 140 mM Cl outside), for an outward-directed Cl gradient (b, 50 mM Cl outside), and for biionic conditions (c, 140 mM iodide outside). The pipette solution contained 145 mM Cl. This experiment demonstrates that the Ca-induced current is a Cl current and that the relative iodide permeability P_I/P_{Cl} of the Ca-activated Cl channels is 3.

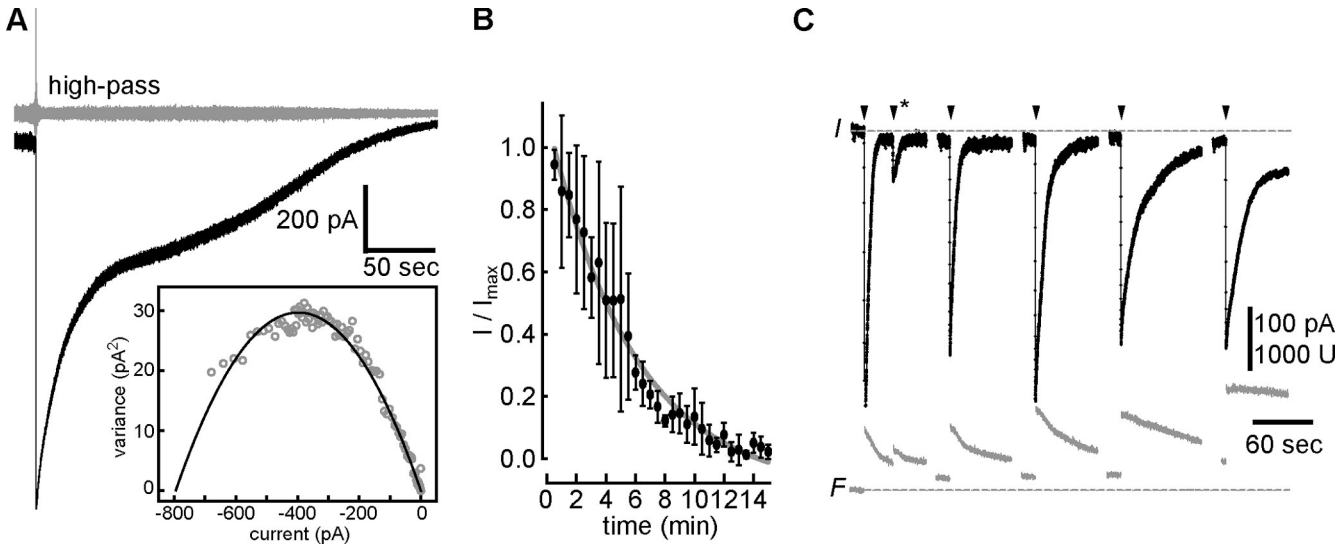

Figure 2. Single channel current and rundown of channel activity in excised patches. (A) Determination of the single-channel current of Ca-activated Cl channels. Ca-dependent Cl current was induced by a 1-s light flash to obtain a high level of intracellular Ca, and recorded at −40 mV during the return of the Ca concentration to submicromolar levels. The variance of the declining current was analyzed after high-pass filtering (2 Hz, gray trace). Current variance was determined after subtraction of the background variance measured upon return to the baseline. Variance analysis (inset) yielded a mean single channel current of 0.15 pA and a channel number of 5323 in this cell. (B) Current recording (mean ± SD of three patches; −40 mV) illustrating the decline of Ca-activated Cl currents in excised inside-out patches. Each point represents the current induced by a 5-s pulse of 67 μM Ca delivered to the cytosolic side of the patch. Blockage by 100 μM niflumic acid confirmed that the currents were conducted by Ca-activated Cl channels (not depicted). The initial current amplitudes were 1–2 pA, corresponding to 10–20 active channels. The current decline is described by a single-exponential function with a time constant of 5.0 min (solid line). (C) Continuous responsiveness of Ca-activated Cl channels in the whole-cell configuration. Intense light flashes (1 s duration) were applied 10 min after breakthrough and then at 10-min intervals (▼). Cl channels responded with phasic activation to each flash, and with tonic activation to the increasing level of free intracellular Ca (gray trace). A repeated flash after 30 s (▼*) was almost ineffective because the pool of caged Ca was exhausted by the preceding 1-s flash and had to be replenished by diffusion from the pipette. The fluorescence recording is interrupted during flash delivery, masking the peaks of the Ca transients during illumination.

preference for iodide (Reisert et al., 2003). To assess the ion selectivity of the *Odora* channels, we compared current-to-voltage (I/V_m) relations before and after photorelease of Ca (Fig. 1 D). The reversal voltage of the net current was 2.1 ± 12 mV (three cells) with 145 mM Cl in the pipette and 140 mM in the bath. Similar to OSN Cl channels, the steady-state I/V_m relation showed only a subtle inward rectification under these near-symmetrical conditions, indicating the virtual absence of voltage-dependent gating. Reducing extracellular Cl to 50 mM (replaced by gluconate) shifted the reversal voltage to 32.6 ± 3.4 mV (three cells), consistent with the theoretical reversal voltage of 27 mV for a perfectly Cl^--sensitive channel. Substituting bath chloride with iodide caused a shift of the reversal voltage to −22.9 ± 3.6 mV (three cells). This result indicates a relative iodide permeability P_I/P_{Cl} of 3.03 ± 0.55 (six cells), close to the value established for native channels (P_I/P_{Cl} of 3.2; Reisert et al., 2003).

To determine the single-channel conductance of the *Odora* channel, we analyzed the variance of the Ca-induced current during the slow decline of the intracellular Ca concentration that follows the photorelease of Ca, as the cell extrudes and sequesters the photoreleased Ca (Fig. 2 A). During that phase, the mean open probability (P_o) of the channels decreases continuously from near unity at high Ca (Reisert et al., 2003) to near zero after removal of free Ca from the cytosol. The current variance σ^2, which arises from the gating activity of the Ca-activated Cl channels, is a parabolic function of the macroscopic current amplitude (Fig. 2 A, inset). Starting near zero when channels are closed ($P_o = 0$), σ^2 peaks at half-maximal activation ($P_o = 0.5$, where gating activity is maximal) and then declines as the channels approach the permanently open state ($P_o = 1$). For a simple two-state (closed/open) channel, the dependence of σ^2 on the mean macroscopic current I, is described by $\sigma^2 = iI - I^2/N$, where N is the number of channels activated by the photoreleased Ca, and i is the single-channel current (Sigworth, 1980). Fitting this equation to the data obtained from Ca-activated Cl currents in *Odora* cells yielded a single-channel current of −0.11 ± 0.05 pA (five cells) at −40 mV, corresponding to a channel conductance of 2.7 pS. The number of channels per cell (*N*) varied from 2,800 to 18,000 (mean: 7,502 ± 5,373). Channels in excised patches from OSNs showed a similarly low conductance of 1.3 pS (−0.05 pA at −40 mV; Reisert et al., 2003).

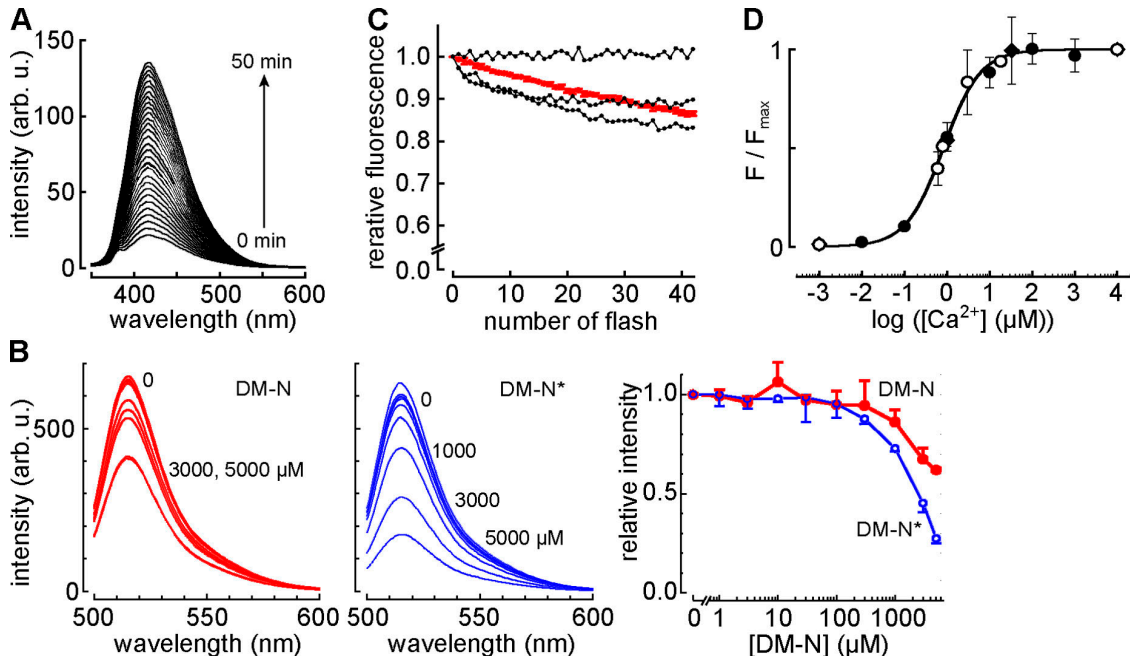

Figure 3. Calibration of Ca-dependent fluorescence in the presence of caged Ca. (A) Increasing fluorescence during progressive photolysis of DM-nitrophen at λ = 340 nm (both for excitation and photolysis). Spectra were obtained from 50 μM DM-nitrophen dissolved in pipette solution. (B) Fluorescence quenching of Ca-saturated fluo-5F by increasing concentrations of caged (DM-N, left) or photoreleased (DM-N*, center) DM-nitrophen (0, 1, 3, 10, 30, 100, 300, 1,000, 3,000, 5,000 μM). The diagram illustrates the higher quenching efficacy of DM-N* at concentrations >100 μM. λ_{exc} = 475 nm. (C) Decline of the fluorescence of Ca-saturated fluo-5F during a series of 50-ms flashes due to the increasing ratio of DM-N*/DM-N. The same flash protocol was used for the determination of Ca sensitivity in this study. Fluorescence quenching causes a ~15% reduction of the signal in cells (black traces) and in cell-free pipette solution (red trace). (D) Calibration of fluo-5F fluorescence. The fluorescence of 20 μM fluo-5F was measured in a series of Ca-standard solutions (●), which was also used to calibrate a Ca electrode. The fluorescence was then measured in two sets of solutions containing either 5 mM DM-N (◆) or 5 mM DM-N* (○), as well as different concentrations of total Ca^{2+}, resulting in the indicated free Ca concentrations ($[Ca^{2+}]$), which were determined using the Ca electrode. The apparent K_D of fluo-5F (0.80–0.84 μM) was not significantly changed by DM-N or DM-N*.

Ca-activated Cl channels in membrane patches excised from OSNs show a pronounced "rundown" phenomenon: The Cl current declines irreversibly after membrane excision within a few minutes (Reisert et al., 2003). In a few membrane patches from *Odora* cells, we were able to record Ca-activated Cl currents (1–2 pA, originating from 10–20 channels) over a prolonged period of time. Repeated, saturating Ca pulses caused progressively smaller current responses until the current was completely lost after 15 min (Fig. 2 B). In between the Ca pulses, the patch was kept for 25 s in Ca-free solution to allow recovery from Ca-dependent inactivation (Reisert et al., 2003). A slow, irreversible rundown developed with a single-exponential time course (time constant: 5.0 min), similar to the rundown observed in membrane patches from OSNs. The reason for the rundown is not clear, but it does not occur in the intact cell. Repeated application of light flashes over 60 min elicited Cl currents with only slightly decreasing amplitude (Fig. 2 C). Thus, the irreversible loss of channel activity seen in both *Odora* cells and OSNs is induced when the channels lose contact with the cytosol.

Ca Sensitivity of Cl Channels

Because channels in *Odora* cells are expressed at low density, and are unstable in excised patches, we had to determine the Ca sensitivity inside *Odora* cells by quantitative evaluation of the current and fluorescence signals. Earlier studies have indicated that caged Ca may interact with fluorescent Ca indicators (Zucker, 1992; Hadley et al., 1993), and we therefore explored this question for our experiments. The ratiometric Ca dyes fura and indo have to be excited in the near UV range (340–380 nm). We found that DM-nitrophen emits fluorescence following photolysis when excited at 340 nm (Fig. 3 A), ruling out fura and indo dyes for our purpose. The excitation wavelength used for fluo-5F (475 nm) did not cause DM-nitrophen fluorescence. However, in solution containing both fluo-5F and DM-nitrophen, the fluorescence of fluo-5F was quenched by DM-nitrophen, and quenching efficiency was stronger after photolysis (Fig. 3 B). Consequently, fluo-5F fluorescence intensity recorded at saturating intracellular Ca decreases progressively during photolysis of caged Ca (Fig. 3 C). DM-nitrophen is used at concentrations of 1–10 mM, so the question arises whether quenching changes the

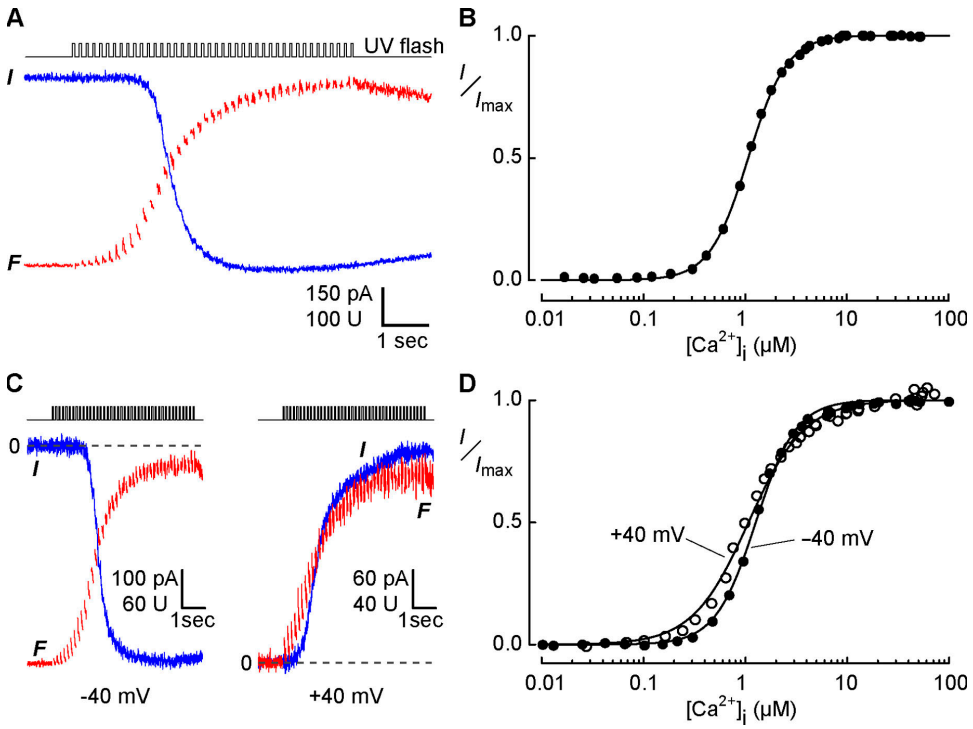

Figure 4. Determination of the Ca sensitivity of Cl channels in an *Odora* cell. (A) Simultaneous current (blue trace) and fluorescence (red trace) recordings at −40 mV during incremental photolysis of caged Ca in an *Odora* cell. A series of 42 flashes (50 ms) with reduced light intensity caused a stepwise increase of the cytosolic Ca concentration that saturated both the Cl channels and the Ca-sensitive dye. (B) Dose–response relation for the activation of Cl channels obtained from the data in A. The Ca concentration for half-maximal activation $K_{1/2}$ was 1.07 μM, with a Hill coefficient of 2.3. (C) Examination of the effect of membrane voltage on Ca sensitivity. The same protocol as in A was applied at −40 mV (left) and at + 40 mV (right). The inward current at −40 mV was generated by Cl efflux, the outward current at +40 mV by Cl influx. The dashed line indicates zero current. (D) Dose–response relation obtained from the data in C, yielding $K_{1/2}$ and n values of 1.27 μM and 2.19 for −40 mV, and 1.07 μM and 1.58 for +40 mV, respectively.

relation between fluo-5F fluorescence and the free Ca concentration. To examine this point, we prepared two sets of solutions with known Ca concentrations (determined using a Ca electrode), one with 5 mM DM-nitrophen before photolysis, and one with the same DM-nitrophen concentration after photolysis. The dependence of fluo-5F fluorescence intensity on free Ca is shown in Fig. 3 D. The Ca concentrations for half-maximal fluorescence were 0.84 ± 0.07 μM (four experiments) in solution without DM-nitrophen, 0.80 ± 0.06 μM (two experiments) with 5 mM DM-nitrophen before photolysis, and 0.84 ± 0.04 μM (two experiments) after photolysis. Thus, DM-nitrophen quenches fluo-5F fluorescence without changing its Ca sensitivity. The presence of caged Ca, therefore, does not compromise the use of fluo-5F as intracellular Ca reporter under our recording conditions.

To measure the Ca sensitivity of Cl channels in *Odora* cells, we induced successive increments of the intracellular Ca concentration by applying a series of 50-ms light flashes. Each flash increased both the Ca-dependent fluorescence intensity and the current amplitude by a measurable step (Fig. 4 A). After converting fluorescence intensity into Ca concentration (see Materials and Methods), the two signals were related in a dose–response plot (Fig. 4 B), which yielded the Ca concentration for half-maximal channel activation, $K_{1/2}$, and the Hill coefficient, n, according to

$$I = I_{max} \frac{[Ca]_i^n}{[Ca]_i^n + K_{1/2}^n}.$$

In the experiment shown in Fig. 4, $K_{1/2}$ was 1.07 μM and n was 2.3. Comparison to the data obtained from native channels at −40 mV (2.2 μM, n = 2.8; Reisert et al., 2003) shows that Ca-activated Cl channels in *Odora* cells and OSNs have a similar Ca sensitivity and cooperativity of activation. The Ca sensitivity of native channels in OSNs displays only a weak voltage sensitivity with a $K_{1/2}$ of 2.2 μM at −40 mV and 1.5 μM at +40 mV (Reisert et al., 2003). To test this point, we measured the Ca sensitivity of the *Odora* channels at these two voltages (Fig. 4 C). The dose–response relations were similar (Fig. 4 D), and the results did not reveal any voltage dependence of activation by Ca (15 cells at −40 mV: $K_{1/2}$ = 1.28 μM ± 0.10 μM, n = 2.08 ± 0.12; 8 cells at +40 mV: $K_{1/2}$ = 1.14 μM ± 0.11 μM, n = 1.66 ± 0.08).

Taken together, our comparison of *Odora* channels and OSN channels demonstrates that both cells express Ca-activated Cl channels with similar functional properties. Since *Odora* cells are derived from the progenitor cells of OSNs in rat olfactory epithelium, it is reasonable to assume that both cells express the same channel protein. It is therefore justified to use *Odora* cells to explore a possible role of CaM in the activation of this channel. While *Odora* cells in the control state are not a suitable

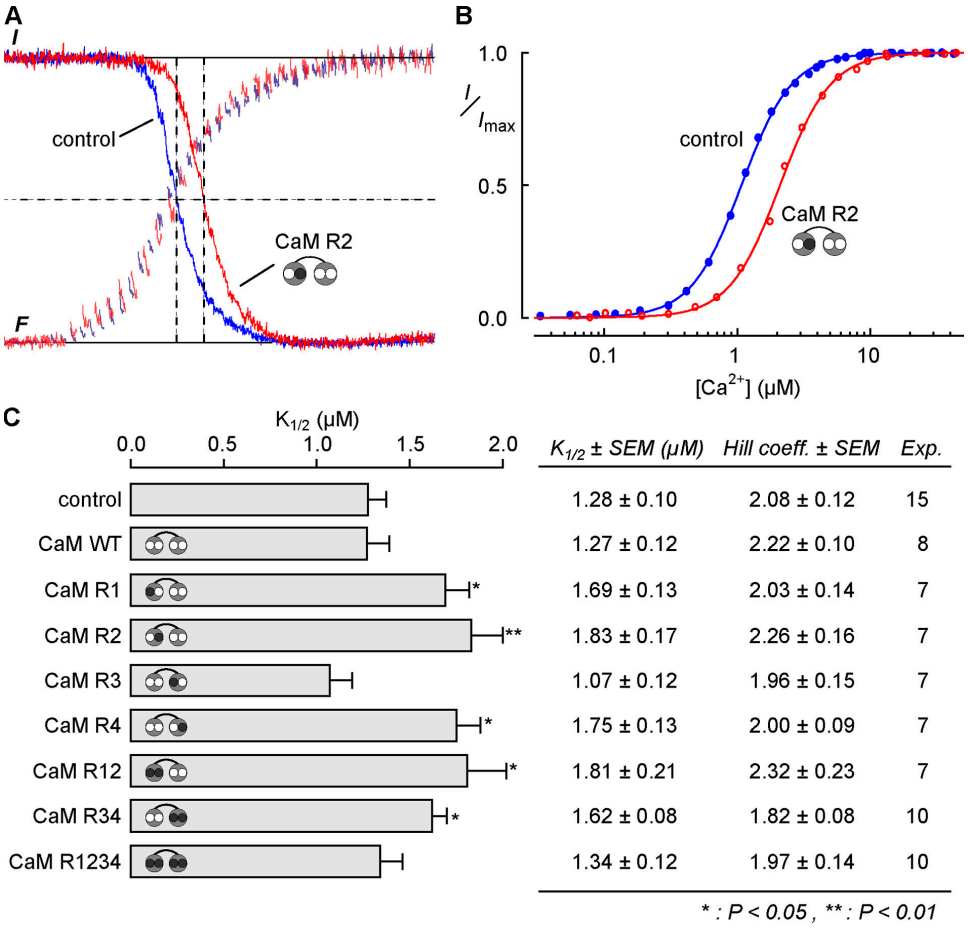

	$K_{1/2}$ ± SEM (μM)	Hill coeff. ± SEM	Exp.
control	1.28 ± 0.10	2.08 ± 0.12	15
CaM WT	1.27 ± 0.12	2.22 ± 0.10	8
CaM R1	1.69 ± 0.13	2.03 ± 0.14	7
CaM R2	1.83 ± 0.17	2.26 ± 0.16	7
CaM R3	1.07 ± 0.12	1.96 ± 0.15	7
CaM R4	1.75 ± 0.13	2.00 ± 0.09	7
CaM R12	1.81 ± 0.21	2.32 ± 0.23	7
CaM R34	1.62 ± 0.08	1.82 ± 0.08	10
CaM R1234	1.34 ± 0.12	1.97 ± 0.14	10

*: $P < 0.05$, **: $P < 0.01$

Figure 5. Effects of mutant calmodulins on the Ca sensitivity of Cl channels. (A) Current and fluorescence recordings from two cells that displayed similar increments of intracellular Ca in response to a flash series. The red traces were recorded from a cell transfected with the mutant CaM R2, in which one of the two NH_2-terminal Ca binding sites is disabled by a point mutation. Note that more flashes (i.e., higher Ca concentrations) are necessary to achieve half-maximal activation in the cell expressing the mutant. Normalized recordings obtained at −40 mV. (B) Dose–response relations derived from the data in A. Transfection with CaM R2 shifted the dose–response curve to the right, increasing $K_{1/2}$ from 1.07 to 2.09 at constant Hill coefficient (n = 2.3). (C) Collected results of transfection experiments with mutant calmodulins. The disabled Ca binding sites are indicated by dark gray dots on the CaM symbols. Asterisks indicate the significance level (nonpaired Student's *t* test) compared with control cells. "Exp." denotes the number of cells examined (two to seven transfections each). Mutations in the Ca binding sites 1, 2, and 4 caused a reduction of Ca sensitivity, while a mutation in binding site 3 was ineffective. The totally inactive mutant CaM R1234 points to a requirement of Ca for the association of CaM with the Cl channel (see Discussion). Ranges for $K_{1/2}$ values were (in μM) as follows. Control, 0.91–1.98; CaM WT, 0.90–2.07; CaM R1, 1.33–2.17; CaM R2, 1.06–2.40; CaM R3, 0.83–1.74; CaM R4, 1.16–2.13; CaM R12, 1.06–2.49; CaM R34, 1.19–1.90; CaM R1234, 0.63–2.05.

model for olfactory transduction as a whole, they are a good source for olfactory Ca-activated Cl channels.

Role of CaM in the Activation of *Odora* Cl Channels

To examine a possible involvement of CaM in the activation of Ca-dependent Cl currents, we transfected *Odora* cells with CaM mutants in which one or several of the four EF-hand Ca binding sites were disabled by a single amino acid exchange. The dominant negative effect of these CaM mutants has been used to reveal the role of CaM in channel gating (Xia et al., 1998; Alseikhan et al., 2002). Fig. 5 A shows how the *Odora* Cl channels are affected by the mutant CaM R2, in which one of the two NH_2-terminal Ca binding sites is disabled (D56A). In a cell transfected with CaM R2, the Ca-dependent Cl current was activated at higher Ca levels than channels in a nontransfected control cell. In contrast, the Ca dependence of currents in cells transfected with wild-type CaM was not different from nontransfected cells (see below). Thus, the mutated Ca binding site of CaM R2 somehow contributes to the Ca sensitivity of the Cl channels. Indeed, the dose–response relation of the Ca-dependent Cl current in CaM R2-transfected cells was shifted to the right (Fig. 5 B), with a twofold increase of $K_{1/2}$ (1.07→2.09 μM) and an unchanged Hill coeffcient (n = 2.3). The reduced Ca sensitivity of channels in the CaM R2-transfected cell suggests that the mutation compromises the gating mechanism. This result is indicative of a gating mechanism in which the effect of Ca on the Cl channel is mediated by CaM.

To find out which of the Ca binding sites of CaM contribute to this process, we used a series of different CaM mutants for transfection of *Odora* cells and derived $K_{1/2}$ values and the Hill coefficients from whole-cell recordings as depicted in Fig. 4. The results of these experiments are summarized in Fig. 5 C and revealed the following points. (a) CaM mutants with disabled Ca binding sites 1, 2, or 4 caused a decrease of the Cl channels' Ca sensitivity. The CaM mutants gave rise to a twofold increase of $K_{1/2}$, but left the Hill coefficient unchanged. (b) Mutation of the COOH-terminal Ca binding site 3 did not affect Ca sensitivity. (c) When all

four Ca binding sites were disabled (CaM R1234), current amplitudes and Ca sensitivity in the transfected cells were not different from untransfected cells, or from cells transfected with wild-type CaM. Successful transfection of CaM R1234 was confirmed by fluorescence imaging using both cotransfection with RFP and the tagged version YFP-CaM R1234. The inability of the inactive CaM mutant to affect the Cl current suggests that this mutant is unable to bind to the channel and, consequently, does not compete with endogenous intact CaM for channel control. In summary, our results demonstrate that CaM participates in the gating control of Ca-activated Cl channels in *Odora* cells.

DISCUSSION

Calmodulin and Ca-activated Cl Channels

A major problem for research into anion-based signal amplification is that the molecular identity of its key protein, the Ca-activated Cl channel, has not been identified. Neither of the two currently examined families of Ca-activated Cl channels, the CLCA family (for review see Loewen and Forsyth, 2005) and the bestrophin family (for review see Hartzell et al., 2005), appear to be promising candidates for the olfactory channel. While electrophysiology revealed that the olfactory channels are concentrated in the ciliary membrane of OSNs (Eberius and Schild, 2001; Reisert et al., 2003), none of the CLCA or bestrophin proteins so far displays a matching expression pattern. Moreover, *Odora* cells do not express *clca* mRNA (unpublished data), and some functional properties of bestrophin channels are not consistent with the OSN channels. Thus, in the absence of evidence for a role of CLCAs and bestrophins in olfactory transduction, it is necessary to examine functional properties of the OSN channels that may lead to its molecular identification. A possible role of CaM in gating control could be useful for that task, because interactions between CaM and the channel can be exploited for protein purification and identification. Various ion channels use CaM as a Ca-sensitive, regulatory subunit (for review see Saimi and Kung, 2002), and engineered CaMs were instrumental in revealing this (Xia et al., 1998; Fanger et al., 1999; Zühlke et al., 1999; DeMaria et al., 2001; Liang et al., 2003; Young and Caldwell, 2005). In these experiments, mutant CaMs were cotransfected with the cDNA of already cloned channels to study the CaM effects on the heterologously expressed proteins. In the present study, we used the CaM mutants to obtain information about an unknown channel protein, information that might lead to its molecular identification. We verified that the *Odora* Cl channels share a distinctive set of functional parameters with the native Cl channels from OSNs, and measured the Ca sensitivity of Cl channels in *Odora* cells expressing mutant CaM. We recorded from cells cotransfected with CaM mutants and with red fluorescent protein as transfection marker. Although we could not measure the amount of mutant CaM protein present in the transfected cells, we assume for three reasons that significant levels were expressed. (1) Overexpression of CaM mutants is a well-established method (e.g., Alseikhan et al., 2002; Liang et al., 2003). (2) Cells transfected with YFP-tagged versions of either wt CaM or CaM R1234 showed bright fluorescence. (3) Transfection with CaM mutants yielded consistent effects on the Cl channels. When the Ca binding sites 1, 2, or 4 of CaM were disabled, we found a roughly twofold increase in $K_{1/2.}$ The same observation (a twofold increase of $K_{1/2}$) is indicative of Ca-CaM–mediated channel gating in SK-type Ca-activated K channels (Keen et al., 1999). In contrast to the SK channels, where only the NH_2- terminal domain of CaM (Ca binding sites 1 and 2) contributes to channel activation, the Ca-activated Cl channels respond to NH_2-terminal and COOH-terminal CaM mutants, suggesting that both lobes of CaM are involved in channel control. A second difference to the SK channel data is that Hill coefficients are not changed by the CaM mutants in Cl channels, and remain close to 2 in all transfections. In SK channels, Hill coefficients drop from 4.6 to 2.6/2.8 if either of the two COOH-terminal Ca binding sites of CaM is disabled (Keen et al., 1999). These observations suggests that Ca binding to CaM contributes to the cooperativity of activation in SK channels, but not in Cl channels. It appears that cooperative activation of the Cl channels reflects allosteric interactions within the channel protein.

Does Ca-CaM bind to the Cl^- channel protein? It is unlikely that the olfactory channels are activated via an indirect action, like Ca-CaM–dependent phosphorylation. Channel activation upon application of saturating Ca steps is too fast (<100 ms) to be consistent with phosphorylation, and channels can be activated in excised patches for >20 min in the absence of ATP (Reisert et al., 2003). Thus, Ca-CaM probably interacts directly with the olfactory Cl channel or, alternatively, with a channel-associated regulatory protein. And the observation that CaM R1234 does not affect the channels points to a Ca dependence of this interaction. The whole-cell currents in the cells transfected with CaM R1234 were not smaller than in control cells, ruling out the possibility that a major fraction of the channels was silenced by association with this mutant. It appears that the integrity of the Ca binding EF hands in at least one of the two lobes of CaM is necessary for interaction, and that both lobes have to be functional for channel activation. The voltage insensitivity of the activation process indicates that the Ca binding sites do not reside within the electrical field across the membrane. In contrast, Ca binding to the pore of cAMP-gated channels is clearly voltage dependent, with a $K_{1/2}$ that changes

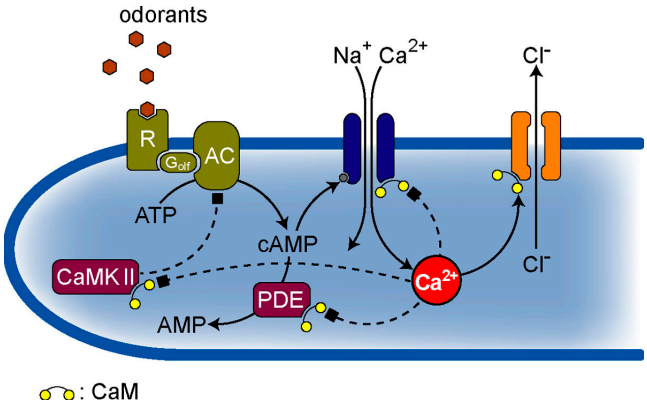

Figure 6. Model for anion-based signal amplification in OSN cilia. Odorants bind to receptor proteins in the ciliary membrane (R). This leads to the synthesis of cAMP through activation of adenylyl cyclase type III (AC) and to opening of Ca-permeable, cAMP-gated transduction channels, which conduct a small primary receptor current. The inflowing Ca induces an excitatory Cl current by opening Ca-CaM–activated Cl channels. This amplifies the primary receptor current about 10-fold because Cl channels outnumber cAMP-gated channels by a factor of eight. Ca also triggers inhibitory processes (dashed lines), including the feedback inhibition of the cAMP-gated channels, the activation of PDE by Ca-CaM, and the inhibition of AC III through phosphorylation by the CaM-dependent protein kinase CaMK II. CaM thus controls the molecular events that generate and terminate the olfactory receptor current.

10-fold over a voltage range of 80 mV (Dzeja et al., 1999). Our observation of voltage insensitivity in the Ca-activated Cl channels is consistent with the notion that Ca binds to an associated regulatory protein outside the membrane. The subtle voltage effect on $K_{1/2}$ seen in excised patches from OSNs (2.2 μM at −40 mV, 1.5 μM at +40 mV; Reisert et al., 2003) may be construed as indicative of a voltage-induced conformational change that facilitates gating at positive membrane voltages.

Our data thus indicate that CaM associates with the olfactory Cl channels or with an adaptor protein, that this interaction requires functional Ca binding sites in the CaM molecule, and that CaM mediates channel activation at micromolar Ca concentrations. In the absence of any structural information (number and type of CaM binding sites, subunit composition, etc.) it is not productive to speculate about the mechanism of channel regulation by Ca-CaM. Our results do not reveal details on the molecular interaction between Ca-activated Cl channels and Ca-CaM, but they demonstrate that the binding of Ca to CaM is a critical step in channel activation.

Calmodulin in the Olfactory Transduction Compartment

The sensory cilia of OSNs represent a distinct transduction compartment, electrically connected to the OSN dendrite, the site of action potential generation (Dubin and Dionne, 1994). A number of studies have revealed that CaM drives regulatory feedback mechanisms that control several key steps of the transduction cascade (Fig. 6). Triggered by Ca influx during odor detection, CaM reduces ciliary cAMP through activation of phosphodiesterase (PDE1C2; Yan et al., 1995) and by inhibition of adenylyl cyclase (AC III), which is a substrate for the CaM-dependent protein kinase CaMK II (Wei et al., 1998). Moreover, CaM desensitizes the cAMP-gated channel to its ligand and thereby promotes channel closure and rapid adaptation (Bradley et al., 2004). In the present paper, we present evidence for the concept that CaM is not only involved in the termination of the receptor current, but also in its generation. Our data from *Odora* cells suggest that CaM may serve as a crucial link between the two transduction channels by coupling a depolarizing Cl current to the odor-induced Ca signal. Our transduction model (Fig. 6) illustrates the dual effect of Ca-CaM. The inhibitory effects of Ca-CaM restrict the activity of the cAMP-gated channels to a short time period. The transient Ca influx during this period causes a prolonged elevation of the ciliary Ca concentration and, hence, the opening of multiple Cl channels, as there are eightfold more Cl channels in the ciliary membrane than cation channels. Consequently, the initial small Ca influx triggers a much larger Cl efflux and generates an excitatory receptor current with Cl as the main charge carrier. Because CaM appears to control both excitatory and inhibitory processes, it will be important to examine the exact temporal characteristics of each component of the regulatory program. The activation of the Cl channels by Ca-CaM is fast and follows the ciliary Ca concentration in the micromolar concentration range (Reisert and Matthews, 2001a). The Cl channels show only modest intrinsic inactivation/desensitization, causing ∼20% current decline within 10 s (Reisert et al., 2003). The time course of PDE activation and AC III inhibition has not been characterized in intact cilia, and it is not known how these processes contribute to shaping the receptor current. In any case, the inhibitory program is designed to terminate the receptor current within a few seconds, even if stimulation persists, and it is completed when Ca is extruded from the cilia and the Cl channels close (Reisert and Matthews, 1998, 2001b). Thus, throughout a "sniff" of a few seconds, CaM appears to integrate the transduction process and to bring about a transient receptor potential in response to an odor stimulus.

Calmodulin and Anion-based Signal Amplification

Why do OSNs need anion-based signal amplification? The odorant receptor proteins that are presented by OSNs on their sensory cilia bind their ligands with only moderate affinity. Indeed, Bhandawat et al. (2005) have demonstrated that the dwell time of an odorant on its receptor is 1 ms or less, and that the chance for activating even a single GTP binding protein within this time period is small. This result is consistent with a large

number of studies, collected by various recording methods over many years, which all point to a rather low odorant sensitivity of OSNs. When applied in aqueous solution, 1–100 μM of odorant is needed to evoke measurable electrical (Firestein et al., 1993) or biochemical (Boekhoff et al., 1990) responses. A recent study of odorant-induced cAMP production in OSNs (Takeuchi and Kurahashi, 2005) has revealed that the metabotropic transduction cascade in olfactory cilia operates with low gain. Working with amphibian OSNs, the authors found that the intracellular cAMP concentration rises at a rate of just a few μM/s at threshold odor concentrations, and reaches a maximum rate of 96 μM/s at saturating odor concentrations. The low sensitivity of OSNs may reflect an evolutionary compromise between the need to detect individual odorants at low concentrations, and the need to detect an essentially unlimited variety of different odorous molecules. Odorant receptors with high ligand sensitivity would be suitable for the former task but unsuitable for the latter. The olfactory system thus operates with sensors that display relatively low odorant sensitivity and low selectivity between individual odorants. The remarkable performance of the olfactory system as a whole, both with respect to its high detection efficiency and to its ability to distinguish between chemically similar odors, results to a large extent from central information processing; it arises from the analysis of complex excitation patterns in the olfactory bulb (Friedrich, 2002; Lledo et al., 2005).

Working with low sensitivity receptors puts serious constraints on the transduction machinery that operates within the sensory cilia. Since the production of the second messenger cAMP is limited by the low efficiency of the initial transduction step, a different amplification process is required downstream of the transduction cascade. The sequential activation of cAMP-gated Ca channels and Ca-gated Cl channels fulfills that role. The cAMP-gated channels induce local ciliary Ca signals in the micromolar range and, hence, activate Ca-dependent Cl channels. By actively accumulating Cl to a steady-state intracellular concentration of ∼50 mM (Kaneko et al., 2004; Nickell et al., 2006), a concentration that is similar to the mucosal Cl concentration in vivo (Reuter et al., 1998), OSNs maintain a Cl equilibrium potential near 0 mV. The resting voltage of the OSN thus constitutes a driving force for Cl efflux that accounts for ∼90% of the depolarizing receptor current (Reisert et al., 2003, 2005).

Taken together, anion-based signal amplification converts small Ca signals into substantial changes of membrane voltage. This mechanism is not restricted to OSNs but also operates in other neurons. Of particular interest are the nociceptive neurons of the dorsal root ganglia (DRG neurons). These neurons work without metabotropic amplification of the primary signal, as their transduction channels are directly driven by heat, chemical, or mechanical stimuli. Transduction channels of DRG neurons are invariably Ca permeable; most DRG neurons express Ca-activated Cl channels (Currie et al., 1995; Kenyon and Goff, 1998; Lee et al., 2005), and they accumulate Cl in somata (Alvarez-Leefmans et al., 2001) and sensory endings (Granados-Soto et al., 2005). Accordingly, pain behavior can be induced in animal models by excitatory Cl currents (Ault and Hildebrand, 1994, Carlton et al., 1999) and attenuated by inhibiting Cl accumulation into the sensory endings (Willis et al., 2004). Moreover, inflammation increases the expression of NKCC1 in nociceptors (Morales-Aza et al., 2004), possibly as a means to increase the amplification gain and to enhance excitability. These findings suggest that DRG neurons employ a similar amplification strategy as OSNs. CaM may exert its dual effect, feedback inhibition of Ca channels combined with activation of Cl channels, in nociceptors in the same way as it does in OSNs. The heat-sensitive transduction channel TRPV1 is subject to CaM-mediated feedback inhibition (Rosenbaum et al., 2004). It appears that CaM plays a similar role in these neurons: it curtails Ca influx and induces excitatory Cl currents.

The presence of anion-based signal amplification in OSNs, DRG neurons, and smooth muscle cells (Leblanc et al., 2005) points to a common solution for cells that have to turn small Ca signals into sizeable depolarizations; Cl accumulation provides the driving force for a depolarizing Cl current that is triggered by a Ca signal. Calmodulin is a central component of this amplification mechanism, as it orchestrates both its excitatory and inhibitory processes.

We thank Dr. Dale Hunter for supplying the *Odora* cells and Dr. David Yue (Johns Hopkins University) for supplying the CaM mutants for this study. We thank Dr. Jon Bradley for his valuable comments on the manuscript.

This work was supported by the Deutsche Forschungsgemeinschaft (FR937/7).

Olaf S. Andersen served as editor.

Submitted: 23 January 2006
Accepted: 25 April 2006

REFERENCES

Ault, B., and L.M. Hildebrand. 1994. $GABA_A$ receptor-mediated excitation of nociceptive afferents in the rat isolated spinal cord-tail preparation. *Neuropharmacology.* 33:109–114.

Alseikhan, B.A., C.D. DeMaria, H.M. Colecraft, and D.T. Yue. 2002. Engineered calmodulins reveal the unexpected eminence of Ca^{2+} channel inactivation in controlling heart excitation. *Proc. Natl. Acad. Sci. USA.* 99:17185–17190.

Alvarez-Leefmans, F.J., M. Leon-Olea, J. Mendoza-Sotelo, F.J. Alvarez, B. Anton, and R. Garduno. 2001. Immunolocalization of the Na^+-K^+-$2Cl^-$ cotransporter in peripheral nervous tissue of vertebrates. *Neuroscience.* 104:569–582.

Bhandawat, V., J. Reisert, and K.-W. Yau. 2005. Elementary response of olfactory receptor neurons to odorants. *Science.* 308:1931–1934.

Boekhoff, I., E. Tareilus, J. Strotmann, and H. Breer. 1990. Rapid activation of alternative second messenger pathways in olfactory cilia from rats by different odorants. *EMBO J.* 9:2453–2458.

Bönigk, W., J. Bradley, F. Müller, F. Sesti, I. Boekhoff, G.V. Ronnett, U.B. Kaupp, and S. Frings. 1999. The native rat olfactory cyclic nucleotide-gated channel is composed of three distinct subunits. *J. Neurosci.* 19:5332–5347.

Bradley, J., W. Bönigk, K.-W. Yau, and S. Frings. 2004. Calmodulin permanently associates with rat olfactory CNG channels under native conditions. *Nat. Neurosci.* 7:705–710.

Carlton, S.M., S. Zhou, and R.E. Coggeschall. 1999. Peripheral $GABA_A$ receptors: evidence for peripheral primary afferent depolarization. *Neuroscience.* 93:713–722.

Currie, K.P.M., J.F. Wooton, and R.H. Scott. 1995. Activation of Ca^{2+}-dependent Cl^- currents in cultured sensory neurones by flash photolysis of DM-nitrophen. *J. Physiol.* 482:291–307.

DeMaria, C.D., T.W. Soong, B.A. Alseikhan, R.S. Alvania, and D.T. Yue. 2001. Calmodulin bifurcates the local Ca^{2+} signal that modulates P/Q-type Ca^{2+} channels. *Nature.* 411:484–489.

Dubin, A., and V.E. Dionne. 1994. Action potentials and chemosensitive conductances in the dendrites of olfactory neurons suggest new features for odor transduction. *J. Gen. Physiol.* 103:181–201.

Dzeja, C., V. Hagen, U.B. Kaupp, and S. Frings. 1999. Ca^{2+} permeation in cyclic nucleotide-gated channels. *EMBO J.* 18:131–144.

Eberius, C., and D. Schild. 2001. Local photolysis using tapered quartz fibres. *Pflügers. Arch.* 443:323–330.

Erickson, M.G., B.A. Alseikhan, B.Z. Peterson, and D.T. Yue. 2001. Preassociation of calmodulin with voltage-gated Ca^{2+} channels revealed by FRET in single living cells. *Neuron.* 31:973–985.

Fanger, C.M., S. Ghandshani, N.J. Logsdon, H. Rauer, K. Kalman, J. Zhou, K. Beckingham, K.G. Chandy, M.D. Cahalan, and J. Aiyar. 1999. Calmodulin mediates calcium-dependent activation of the intermediate conductance K_{Ca} channel *IKCa1*. *J. Biol. Chem.* 274:5746–5754.

Firestein, S., C. Picco, and A. Menini. 1993. The relation between stimulus and response in olfactory receptor cells of the tiger salamander. *J. Physiol.* 468:1–10.

Friedrich, R.W. 2002. Real-time odor representation. *Trends Neurosci.* 25:487–489.

Frings, S. 2001. Chemoelectrical signal transduction in olfactory sensory neurons of air-breathing vertebrates. *Cell. Mol. Life Sci.* 58:510–519.

Granados-Soto, V., C.F. Arguelles, and F.J. Alvarez-Leefmans. 2005. Peripheral and central antinociceptive action of Na^+-K^+-2Cl^- cotransporter blockers on formalin-induced nociception in rats. *Pain.* 114:231–238.

Hadley, R.W., M.S. Kirby, W.J. Lederer, and J.P. Kao. 1993. Does the use of DM-nitrophen, nitr-5, or diazo-2 interfere with the measurement of indo-1 fluorescence? *Biophys. J.* 65:2537–2546.

Hartzell, C., I. Putzier, and J. Arreola. 2005. Calcium-activated chloride channels. *Annu. Rev. Physiol.* 67:719–758.

Kaneko, H., I. Putzier, S. Frings, U.B. Kaupp, and T. Gensch. 2004. Chloride accumulation in mammalian olfactory sensory neurons. *J. Neurosci.* 24:7931–7938.

Keen, J.E., R. Khawale, D.L. Farrens, T. Neelands, A. Rivard, C.T. Bond, A. Janowsky, B. Fakler, J.P. Adelman, and J. Maylie. 1999. Domains responsible for constitutive and Ca^{2+}-dependent interactions between calmodulin and small conductance Ca^{2+}-activated potassium channels. *J. Neurosci.* 19:8830–8838.

Kenyon, J.L., and H.R. Goff. 1998. Temperature-dependence of Ca^{2+} current, Ca^{2+}-activated Cl^- current and Ca^{2+} transients in sensory neurons. *Cell Calcium.* 24:35–48.

Kleene, S.J. 1993. Origin of the chloride current in olfactory transduction. *Neuron.* 11:123–132.

Kleene, S.J. 1997. High-gain, low-noise amplification in olfactory transduction. *Biophys. J.* 73:1110–1117.

Kleene, S.J., and R.C. Gesteland. 1991. Calcium-activated chloride conductance in frog olfactory cilia. *J. Neurosci.* 11:3624–3629.

Kurahashi, T., and K.-W. Yau. 1993. Co-existence of cationic and chloride components in odorant-induced current of vertebrate olfactory receptor cells. *Nature.* 363:71–74.

Leblanc, N., J. Ledoux, S. Saleh, A. Sanguinetti, J. Angermann, K. O'Driscoll, F. Britton, B.A. Perrino, and I.A. Greenwood. 2005. Regulation of calcium-activated chloride channels in smooth muscle cells: a complex picture is emerging. *Can. J. Physiol. Pharmacol.* 83:541–556.

Lee, M.G., D.W. MacGlashan, and B.J. Undem. 2005. Role of chloride channels in bradykinin-induced guinea pig airway vagal C-fibre activation. *J. Physiol.* 566:205–212.

Liang, H., C.D. DeMaria, M.G. Erickson, M.X. Mori, B.A. Alseikhan, and D.T. Yue. 2003. Unified mechanisms of Ca^{2+} regulation across the Ca^{2+} channel familiy. *Neuron.* 39:951–960.

Lledo, P.M., G. Gheusi, and J.D. Vincent. 2005. Information processing in the mammalian olfactory system. *Physiol. Rev.* 85: 281–317.

Loewen, M.E., and G.W. Forsyth. 2005. Structure and function of CLCA proteins. *Physiol. Rev.* 85:1061–1092.

Lowe, G., and G.H. Gold. 1993. Nonlinear amplification by calcium-dependent chloride channels in olfactory receptor cells. *Nature.* 366:283–286.

Morales-Aza, B.M., N.L. Chillingworth, J.A. Payne, and L.F. Donaldson. 2004. Inflammation alters cation chloride cotransporter expression in sensory neurons. *Neurobiol. Dis.* 17:62–69.

Murrell, J.R., and D.D. Hunter. 1999. An olfactory sensory neuron line, *Odora*, properly targets olfactory proteins and responds to odorants. *J. Neurosci.* 19:8260–8270.

Nakamura, T., and G.H. Gold. 1987. A cyclic nucleotide-gated conductance in olfactory receptor cilia. *Nature.* 325:442–444.

Nickell, W.T., N.K. Kleene, R.C. Gesteland, and S.J. Kleene. 2006. Neuronal chloride accumulation in olfactory epithelium of mice lacking NKCC1. *J. Neurophysiol.* 95:2003–2006.

Oh, E.J., and D. Weinreich. 2004. Bradykinin decreases K^+ and increases Cl^- conductances in vagal afferent neurones of the guinea pig. *J. Physiol.* 558:513–526.

Reisert, J., P.J. Bauer, K.-W. Yau, and S. Frings. 2003. The Ca-activated Cl channel and its control in rat olfactory receptor neurons. *J. Gen. Physiol.* 122:349–363.

Reisert, J., J. Lai, K.-W. Yau, and J. Bradley. 2005. Mechanism of the excitatory Cl^- response in mouse olfactory receptor neurons. *Neuron.* 45:553–561.

Reisert, J., and H.U. Matthews. 1998. Na^+-dependent Ca^{2+} extrusion governs response recovery in frog olfactory receptor cell. *J. Gen. Physiol.* 112:529–535.

Reisert, J., and H.U. Matthews. 2001a. Simultaneous recording of receptor current and intraciliary Ca^{2+} concentration in salamander olfactory receptor cells. *J. Physiol.* 535:637–645.

Reisert, J., and H.U. Matthews. 2001b. Response to prolonged odour stimulation in frog olfactory receptor cells. *J. Physiol.* 534: 179–191.

Reuter, D., K. Zierold, W. Schröder, and S. Frings. 1998. A depolarizing chloride current contributes to chemo-electrical transduction in olfactory sensory neurons *in situ*. *J. Neurosci.* 18:6623–6630.

Rosenbaum, T., A. Gordon-Shaag, M. Munari, and S.E. Gordon. 2004. Ca^{2+}/calmodulin modulates TRPV1 activation by capsaicin. *J. Gen. Physiol.* 123:53–62.

Saimi, Y., and C. Kung. 2002. Calmodulin as an ion channel subunit. *Annu. Rev. Physiol.* 64:289–311.

Sigworth, F.J. 1980. The variance of sodium current fluctuations at the node of Ranvier. *J. Physiol.* 307:97–129.

Takeuchi, H., and T. Kurahashi. 2005. Mechanisms of signal amplification in the olfactory sensory cilia. *J. Neurosci.* 25:11084–11091.

Wei, J., A.Z. Zhao, G.C. Chan, L.P. Baker, S. Impey, J.A. Beavo, and D.R. Storm. 1998. Phosphorylation and inhibition of adenylyl cyclase by CaM kinase II in neurons: a mechanism for attenuation of olfactory signals. *Neuron.* 21:495–504.

Willis, E.F., G.F. Clough, and M.K. Church. 2004. Investigation into the mechanisms by which nedocromil, furosemide and bumetanide inhibit the histamin-induced itch and flare response in human skin *in vivo*. *Clin. Exp. Allergy.* 34:450–455.

Xia, X.-M., B. Fakler, A. Rivard, G. Wayman, T. Johnson-Pais, J.E. Keen, T. Ishii, B. Hirschberg, C.T. Bond, S. Lutsenko, et al. 1998. Mechanism of calcium gating in small-conductance calcium-activated potassium channels. *Nature.* 395:503–507.

Yan, C., A.Z. Zhao, J.K. Bentley, K. Loughney, K. Ferguson, and J.A. Beavo. 1995. Molecular cloning and characterization of a calmodulin-dependent phosphodiesterase enriched in olfactory sensory neurons. *Proc. Natl. Acad. Sci. USA.* 92:9677–9681.

Young, K.A., and J.H. Caldwell. 2005. Modulation of skeletal and cardiac voltage-gated sodium channels by calmodulin. *J. Physiol.* 565:349–370.

Zheng, J., and W.N. Zagotta. 2004. Stoichiometry and assembly of olfactory cyclic nucleotide-gated channels. *Neuron.* 42:411–421.

Zühlke, R.D., G.S. Pitt, K. Deisseroth, R.W. Tsien, and H. Reuter. 1999. Calmodulin supports both inactivation and facilitation of L-type calcium channels. *Nature.* 399:159–162.

Zucker, R.S. 1992. Effects of photolabile calcium chelators on fluorescent calcium indicators. *Cell Calcium.* 13:29–40.